Available online at www.sciencedirect.com
SCIENCE DIRECT®
Journal of Chromatography A, 1044 (2004) 287–294
JOURNAL OF CHROMATOGRAPHY A
www.elsevier.com/locate/chroma

# Influence of moderate Joule heating on electroosmotic flow velocity, retention, and efficiency in capillary electrochromatography

Guofang Chen [a,b], Ulrich Tallarek [b], Andreas Seidel-Morgenstern [b], Yukui Zhang [a,*]

[a] *National Chromatographic R & A Center, Dalian Institute of Chemical Physics, Chinese Academy of Sciences, Dalian 116011, China*
[b] *Institut für Verfahrenstechnik, Otto-von-Guericke-Universität Magdeburg, Universitätsplatz 2, 39106 Magdeburg, Germany*

Available online 20 June 2004

**Abstract**

The influence of Joule heating on electroosmotic flow velocity, the retention factor of neutral analytes, and separation efficiency in capillary electrochromatography was investigated theoretically and experimentally. A plot of electrical current against the applied electrical field strength was used to evaluate the Joule heating effect. When the mobile phase concentration of Tris buffer exceeded 5.0 mM in the studied capillary electrochromatography systems using particulate and monolithic columns (with an accompanying power level of heat dissipation higher than 0.35 W/m), the Joule heating effect became clearly noticeable. Theoretical models for describing the variation of electroosmotic flow velocity with increasing applied field strength and the change of retention factors for neutral analytes with electrical field strength at higher Tris buffer concentrations were analyzed to explain consequences of Joule heating in capillary electrochromatography. Qualitative agreement between experimental data and implications of the theoretical model analysis was observed. The decrease of separation efficiency in capillary electrochromatography with macroporous octadecylsilica particles at high buffer concentration can be also attributed to Joule heating mainly via the increased axial diffusion of the analyte molecules and dispersion of solute bands by a nonuniform electroosmotic flow profile over the column cross-section. However, within a moderate temperature range, the contribution of the macroscopic velocity profile in the column arising from radial temperature gradients is insignificant.


*Keywords:* Joule heating; Electroosmotic flow; Retention factor; Efficiency; Benzenes; Benzoates

## 1. Introduction

Capillary electrochromatography (CEC) is a promising separation technique due to its relatively high separation efficiency compared with high-performance liquid chromatography (HPLC) and better selectivity as compared to capillary zone electrophoresis (CZE). In CEC, the mobile phase is electroosmotically driven through the chromatographic bed by an externally applied electrical field. Despite many advantages of CEC that have been demonstrated, some limitations have delayed the widespread acceptance of this potentially powerful separation technique. One of the main limitations regarding performance in CEC arises from Joule heating in the liquid electrolyte. It is well known that Joule heating is generated when a voltage is applied across conductive liquid. The heat generated in the electrolyte solution within the capillary needs to be transported toward the capillary outer wall through the fused silica material of the capillary and then to the surrounding air with forced air convection or cooling liquid. Effective heat dissipation is critical for reproducible and efficient separations in an electrokinetically-driven separation system. Joule heating not only can cause average temperature increase, but also may create a temperature gradient over the cross-section of the capillary with maximum temperature in the center. The variation in the temperature of the mobile phase inside the column and the presence of temperature gradients would have an impact on the electroosmotic flow (EOF), retention kinetics (also on the retention factors themselves), diffusion of analytes, and ultimately on the efficiency and reproducibility of a separation. Further, the temperature change due to Joule heating could lead to bubble formation in the frits or in column sections which may cause disruption of the continuum of electrolyte leading to break down of electrical circuit (current dropping to zero or close to zero values) and, in turn, the CEC operation [1,2]. In addition, temperature rises due to the Joule

* Corresponding author. Tel./fax: +86 411 83693427.
*E-mail address:* ykzhang@dicp.ac.cn (Y. Zhang).

0021-9673/$ – see front matter © 2004 Elsevier B.V. All rights reserved.
doi:10.1016/j.chroma.2004.05.054

heating effect may also lead to the decomposition of thermally labile samples.

Theoretical, as well as experimental studies of the Joule heating and its effect on sample separation have been reported in the literature [3–17]. Knox [3] derived an empirical equation that allows to estimate the plate height contribution arising from the thermal effects. Knox and McCormack [4,5] followed different procedures to calculate the mean temperature change due to Joule heating. Rathore et al. [6] made a thorough investigation of Joule heating in packed capillaries used in CEC with the assumption that the packing particles do not conduct heat and heat transfer occurs solely via the mobile phase flowing through the system. In their study a plot of conductivity, instead of electrical current, versus the applied voltage indicates poor dissipation of the developed heat. Tang et al. [7] carried out a systematic study of the Joule heating effect on EOF and mass transport in a microcapillary using a mathematical model which includes the Poisson–Boltzmann equation, modified Navier–Stokes equations and energy equation coupled through the temperature-dependent liquid dielectric constant, viscosity, and thermal conductivity. Keim and Ladisch [8] presented a two-dimensional transient temperature model for electrochromatography with large-diameter columns. Pulsed magnetic-field gradient nuclear magnetic resonance (NMR) [15], NMR thermometry [16], and Raman spectroscopic measurements [17] have been utilized to measure temperature inside open or packed capillaries. Swinney et al. [12] studied Joule heating in chip-scale capillary electrophoresis using a novel, picoliter volume interferometer.

In the present study, a very simple model based on the Helmholtz–Smoluchowski equation has been utilized to interpret measured results concerning EOF velocity at increasing applied electrical field strength under the influence of Joule heating via the temperature-dependent liquid dielectric constant, viscosity and zeta-potential in CEC. Further, on the basis of the model for the effect of Joule heating on the conductivity proposed by Davis and coworkers [18,19] and the linear relationship between buffer conductivity and temperature, a simple model was put forward to estimate the rise in temperature with increasing field strength under the Joule heating effect. Combined with the van't Hoff equation, an expression for the Joule heating effect on the retention factor was constructed. Finally, the influence of Joule heating on separation efficiency in CEC was also verified experimentally.

## 2. Experimental

### 2.1. Chemicals and materials

Thiourea, tris(hydroxymethyl)aminomethane (Tris) and hydrochloric acid of analytical grade, as well as HPLC grade acetonitrile were purchased from Fluka (Sigma–Aldrich Chemie, Taufkirchen, Germany). The alkylbenzoates and alkylbenzenes came from Merck (Darmstadt, Germany). The materials for monolithic column preparation such as ethylene dimethacrylate (EDMA), butyl methacrylate (BMA), 2-acryloylamido-2-methylpropane-sulfonic acid (AMPS), 3-(trimethoxylsilyl)propyl methacrylate and 1,4-butanediol were obtained from Fluka (Steinheim, Germany). Stationary phases employed in this study, Purospher STAR 400-ODS ($d_p = 2.45\,\mu m$) and Purospher STAR 1200-ODS ($d_p = 2.46\,\mu m$) were a gift from Merck.

A stock solution of 0.5 M Tris (base form) was prepared in Milli-Q water and adjusted to pH 8.30 by titration with concentrated hydrochloric acid. Appropriate volumes of the Tris stock solution, Milli-Q water, and acetonitrile were then mixed to yield the mobile phase containing 80% (v/v) acetonitrile and different effective buffer concentrations, namely 0.1, 0.2, 0.5, 1, 2, 5, 10, 15, 20, 40 and 100 mM. All mobile phase solutions were filtered over a 0.45 μm nylon membrane filter and degassed by sonification prior to use.

### 2.2. Column preparation

As reported in the literature for the preparation of packed capillary columns [20], fused-silica capillaries (100 μm i.d. × 360 μm o.d.; Polymicro Technologies, Phoenix, AZ, USA) were packed by a modified slurry packing technique using a WellChrom pneumatic pump K-1900 (Knauer, Berlin, Germany). The monolithic columns with 75 μm i.d. were fabricated following the procedure described in the literature [21].

### 2.3. Instrumentation

CEC experiments (at controlled ambient temperature of 298 K) with electrical potential gradients between both ends of a duplex column of up to 30 kV were performed in a HP$^{3D}$CE capillary electrophoresis instrument (Agilent Technologies, Waldbronn, Germany) employing the standard forced air-cooling and a diode array detector that was operated at 215 nm. An external helium pressure of 10 bar was applied on both inlet and outlet mobile phase vials for minimizing bubble formation. Samples were injected electrokinetically (3 kV for 3 s). EOF velocities were calculated using the effective column length and residence time distributions of an unretained, uncharged EOF marker (thiourea) which is transported through the packed column by molecular diffusion and the EOF.

## 3. Results and discussion

### 3.1. Ohm plots for evaluating Joule heating

It is well established that there exists a linear relationship between current and applied electrical field strength in the absence of Joule heating in that the conductivity of mobile phase is a constant. In CE or CEC separation systems, an

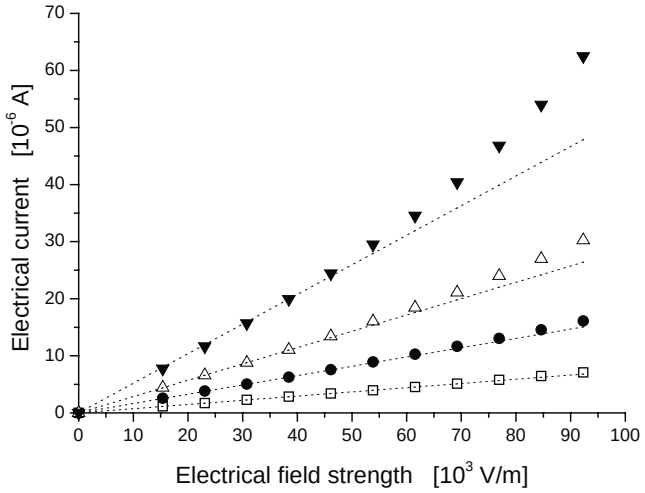


Fig. 1. Dependence of electrical current on applied electrical field strength. Column: 32.5 cm (24 cm effective), Purospher STAR 400-ODS ($d_p$ = 2.45 μm); the mobile phase is acetonitrile–Tris (pH 8.3) (80:20, v/v) with 5 mM (□), 10 mM (●), 20 mM (△), and 40 mM (▼) effective Tris concentration. Dotted lines refer to Ohm plots without Joule heating effect, extrapolated from data at low field strength.

Ohm plot (electrical current versus field strength) is often used to evaluate heating effects in the column, and a positive deviation from linearity in such plots is indicative of significant Joule heating in the systems investigated.

Fig. 1 shows a series of Ohm plots for a packed column in CEC with various buffer concentrations. At increasing ionic strength the extent of a positive deviation from the linearity increases, and for 40 mM Tris buffer concentration the nonlinear dependence of electrical current on applied field strength is clearly manifested.

### 3.2. Effect of Joule heating on electroosmotic flow velocity

In the absence of Joule heating, the macroscopic velocity profile over the column cross-section is more uniform. In the presence of Joule heating the mobile phase temperature will increase resulting in a lower liquid viscosity, higher dielectric constant and higher zeta-potential of the CEC stationary phase which, in turn, leads to an increase in the EOF velocity. However, as mentioned before, Joule heating not only causes a temperature increase, but may also create a significant temperature gradient over the cross-section of the capillary with maximum temperature in the center. The steady-state radial temperature rise in the column can be estimated by [8].

$$T_r = Kr_0^2\left[1-\left(\frac{r}{r_0}\right)^2\right]+T_0 \tag{1}$$

where $T_r$ is the temperature at any radial position ($r$), $T_0$ is the temperature of the column wall, $r_0$ is the column radius, and $K$ is a coefficient related to the heat intensity, thermal conductivity of the fluid in the packed bed, and applied electrical field strength. It should be noted that $K$ is proportional to the square of the electrical field strength:

$$K = hE^2 \tag{2}$$

where $h$ is constant under a given set of experimental conditions. When the magnitude of $\Delta T = T_r - T_0$ is not very large, the temperature dependence of the zeta-potential ($\zeta$), relative dielectric constant ($\varepsilon_r$), and viscosity ($\eta$) may be approximated by the following expressions:

$$\zeta = \zeta_0 \exp(l\,\Delta T) \tag{3}$$

$$\varepsilon_r = \varepsilon_{r,0} \exp(m\,\Delta T) \tag{4}$$

$$\eta = \eta_0 \exp(n\,\Delta T) \tag{5}$$

where $\zeta_0$, $\varepsilon_{r,0}$ and $\eta_0$ refer to the zeta-potential, relative dielectric constant and viscosity at $T_0$; $l$, $m$ and $n$ are constants. In the thin electrical double layer limit (i.e., for pore sizes much larger than the electrical double layer thickness), the average EOF velocity can be calculated from the Helmholtz–Smoluchowski equation [22]:

$$u_{eo} = \frac{\varepsilon_0\varepsilon_r\zeta E}{\eta} \tag{6}$$

Thus, combining Eqs. (1)–(6), the EOF velocity then can be expressed as follows:

$$u_{eo} = \frac{\varepsilon_0\varepsilon_{r,0}\zeta_0 E}{\eta_0}\exp\left\{h(l+m-n)r_0^2\left[1-\left(\frac{r}{r_0}\right)^2\right]E^2\right\} \tag{7}$$

For convenience, we use constants $L$, $M$, and $N$, respectively, instead of $\varepsilon_0\varepsilon_{r,0}\zeta_0/\eta_0$, $hr_0^2(l+m-n)$ and $h(n-l-m)$. With this notation Eq. (7) becomes:

$$u_{eo} = LE\exp(ME^2)\exp(NE^2r^2) \tag{8}$$

In order to further simplify the calculation of $u_{eo}$ the term $\exp(NE^2r^2)$ in Eq. (8) is substituted by $E^\theta$ (where $\theta$ refers to a constant). As a result, the expression for $u_{eo}$ can be rewritten as:

$$u_{eo} = LE^{1+\theta}\exp(ME^2) \tag{9}$$

Eq. (9) can be considered as a general expression for the EOF velocity on account of the Joule heating effect, which clearly shows that there exists a nonlinear relationship between the EOF velocity and the applied electrical field strength. In Eq. (9), the parameter $L = \varepsilon_0\varepsilon_{r,0}\zeta_0/\eta_0$ can be used for extrapolation of the EOF velocity, artificially excluding the Joule heating effect, while parameters $M$ and $\theta$ quantify the contribution of the Joule heating.

Fig. 2 shows the dependence of EOF velocity on applied electrical field strength at an effective Tris buffer concentration of 40 mM which is fitted well by Eq. (9) as:

$$u_{eo} = 0.02444E^{1-0.00409}\exp(0.00001E^2) \tag{10}$$

Here the linear relationship following $u_{eo} = 0.02444E$ demonstrates the dependence of EOF velocity on applied

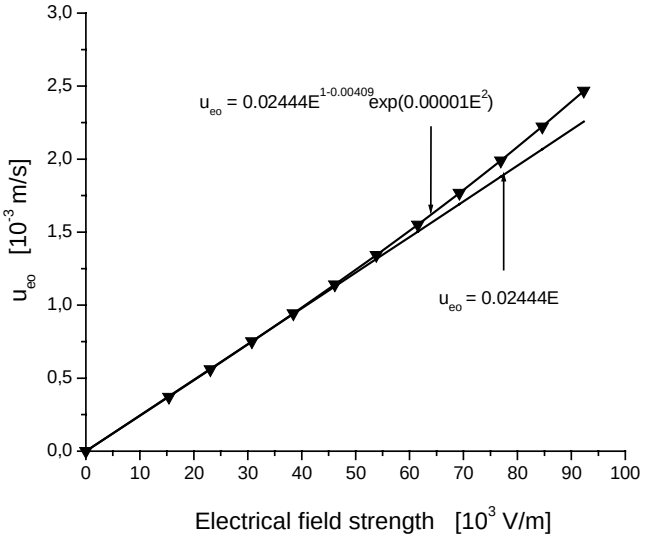


Fig. 2. Electroosmotic flow (EOF) velocity vs. the applied electrical field strength. Same experimental conditions as in Fig. 1; the effective Tris concentration is 40 mM.

electrical field strength, $E$, without the influence of any Joule heating.

In CEC with particulate capillary columns composed of a packed bed and an open tubular segment, the electrical potential does not drop uniformly across the column length, but varies with the local resistance. In order to estimate an authentic EOF mobility in the packed bed, we followed the experimental approach put forward by Rathore and Horváth [23]. As a result, about 90% of the total voltage drop occurs over the packed Purospher STAR 400-ODS column segment, which is therefore taken for a calculation of electroosmotic mobilities ($\mu_{eo}$). Fig. 3 presents $\mu_{eo}$ as a function of the Tris buffer concentration in CEC using macroporous octadecylsilica particles with and without consideration of the

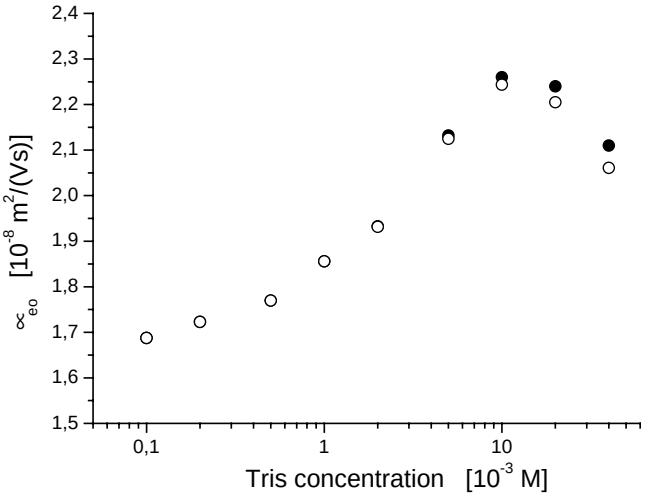


Fig. 3. Comparison of electroosmotic mobilities with (○) and without (●) Joule heating effect (same conditions as in Fig. 1 except for the applied voltage: 20 kV).

Joule heating effect. Here it is worth mentioning that points in Fig. 3 including the influence of the Joule heating are experimental results, while the (estimated) values without a consideration of the Joule heating are acquired based on the parameter $L$ in Eq. (9). It can be seen that under the actual conditions the effect of Joule heating on the electroosmotic mobility becomes noticeable as the Tris buffer concentration exceeds 5.0 mM. Further, the dependence of EOF mobility in beds of porous particles on the mobile phase ionic strength basically is a consequence of the following contributions [20]: (i) usual electrical double layer behaviour at the external particle surface leading to a continuous decrease of the velocity at increasing ionic strength, (ii) generation of intraparticle EOF which increases with ionic strength, and (iii) intraparticle porosity via the dipole coefficient of a porous sphere (independent of ionic strength). Thus, the perfusive EOF is responsible for the increasing EOF mobility at lower ionic strengths, while the first contribution dominates overall mobility at higher ionic strengths leading to an intermediate maximum (Fig. 3).

### 3.3. Effect of Joule heating on retention

Joule heating in CEC arises from the electrical work done by passing an electrical current through a resistive buffer solution in packed beds which results in an increase of the temperature in the electrolyte. The column temperature due to this Joule heating can be approximated with the temperature dependence of electrical conductivity. The buffer conductivity ($\sigma$) depends linearly on temperature [24]:

$$\sigma = \sigma_0[1 + \alpha(T - T_0)] \tag{11}$$

where $T$ is the absolute temperature of the buffer solution in the column, $\alpha$ is the thermal coefficient of conductivity, and $\sigma_0$ is the conductivity measured at a reference temperature ($T_0$). Furthermore, Joule heating caused by power dissipation at higher voltages leads to an increase in electrical conductivity of the mobile phase which has been approximated as [18,19]:

$$\sigma = \sigma_0 + a' E^i \tag{12}$$

where $a'$ and $i$ are constants. When combined with Eq. (11) the relationship between column temperature and applied electrical field strength becomes:

$$T = T_0 + \frac{a' E^i}{\alpha \sigma_0} \tag{13}$$

In chromatographic systems (including electrochromatography), the contribution of temperature to the retention can be described by the van't Hoff equation. In other words, there is a linear relationship between the logarithm of retention factor ($k'$) and reciprocal value of absolute temperature:

$$\ln k' = a + \frac{b}{T} \tag{14}$$

where $a$ and $b$, respectively, are constants which are closely related to the standard entropy and standard enthalpy of

transfer of the solute between phases. Based on Eq. (14), the relationship between retention factors at two different temperatures $T$ and $T_0$ can be analyzed by:

$$\ln\frac{k'_0}{k'} = b\left(\frac{1}{T_0} - \frac{1}{T}\right) \quad (15)$$

When combined with Eq. (13), this equation is transformed into:

$$\ln\frac{k'_0}{k'} = \frac{(a'b/\alpha\sigma_0)E^i}{T_0{}^2 + (a'T_0/\alpha\sigma_0)E^i} \quad (16)$$

By choosing 298 K as the reference temperature ($T_0$), we obtain:

$$\frac{1}{\ln\left(k'_0/k'\right)} = \frac{8.9\times10^4}{A}E^{-i} + B \quad (17)$$

where $A = a'b/\alpha\sigma_0$ and $B = 298/b$. Eq. (17) describes the dependence of the retention factor of a solute on applied electrical field strength with Joule heating.

The electrical field strength dependency of the retention factors for alkylbenzenes in CEC with a polymethacrylate ester-based monolithic column can be seen in Table 1. As the electrical field strength increases, the retention factors of the alkylbenzenes decrease steadily. Table 2 illustrates the relationship between retention factors for alkylbenzoates and applied field strength in CEC with particulate stationary phase. It is clear that the retention factors of methyl- and ethylbenzoate decrease with increasing electrical field strength and the actual level of heat dissipation in the capillary. For example, as the field strength increases from 15.4 to 92.3 kV/m, retention factors for the benzoates decrease by about 17%. The behaviour shown in Tables 1 and 2 can be attributed to the Joule heating effect.

Moreover, with the assumption that there is no significant Joule heating at the smallest field strength, the retention factor under these conditions can be viewed as $k'_0$, and the experimental data in Tables 1 and 2 were transformed into plots of $1/\ln(k'_0/k')$ versus electrical field strength (Figs. 4 and 5). Then, Eq. (17) was used to analyze the curves shown in Figs. 4 and 5. The fitting parameters $A$, $i$ and $B$ are provided in Table 3. The parameter $B = 298/b$ represents the

Table 1
Effect of the applied electrical field strength on retention factors of alkylbenzenes in monolithic CEC

| $E$ (kV/m) | Retention factor | | | | |
|---|---|---|---|---|---|
| | Benzene | Toluene | Propylbenzene | Butylbenzene | Amylbenzene |
| 22.22 | 0.661 | 0.788 | 1.173 | 1.469 | 1.818 |
| 29.63 | 0.653 | 0.778 | 1.156 | 1.447 | 1.792 |
| 37.04 | 0.649 | 0.774 | 1.151 | 1.441 | 1.783 |
| 44.44 | 0.648 | 0.773 | 1.149 | 1.439 | 1.780 |
| 55.56 | 0.642 | 0.766 | 1.138 | 1.426 | 1.766 |
| 66.67 | 0.638 | 0.761 | 1.130 | 1.417 | 1.754 |
| 77.78 | 0.632 | 0.753 | 1.121 | 1.404 | 1.737 |

*Conditions*: Polymethacrylate ester-based monolith column, 27 cm (20 cm effective); mobile phase is acetonitrile–Tris (pH 8.7) (80:20, v/v) with an effective Tris concentration of 5 mM.

Table 2
Effect of the applied electrical field strength on retention factors for alkylbenzoates in particulate CEC

| $E$ (kV/m) | Retention factor | |
|---|---|---|
| | Ethylbenzoate | Butylbenzoate |
| 23.08 | 0.100 | 0.138 |
| 30.77 | 0.099 | 0.137 |
| 38.46 | 0.098 | 0.135 |
| 46.15 | 0.097 | 0.133 |
| 53.85 | 0.095 | 0.130 |
| 61.54 | 0.094 | 0.129 |
| 69.23 | 0.091 | 0.124 |
| 76.92 | 0.088 | 0.121 |
| 84.62 | 0.086 | 0.117 |
| 92.31 | 0.084 | 0.115 |

*Conditions*: Column (32.5 cm, 24 cm effective) of Purospher STAR 400-ODS ($d_p$ = 2.45 μm); mobile phase is acetonitrile–Tris (pH 8.30) (80:20, v/v) with effective Tris concentration of 40 mM.

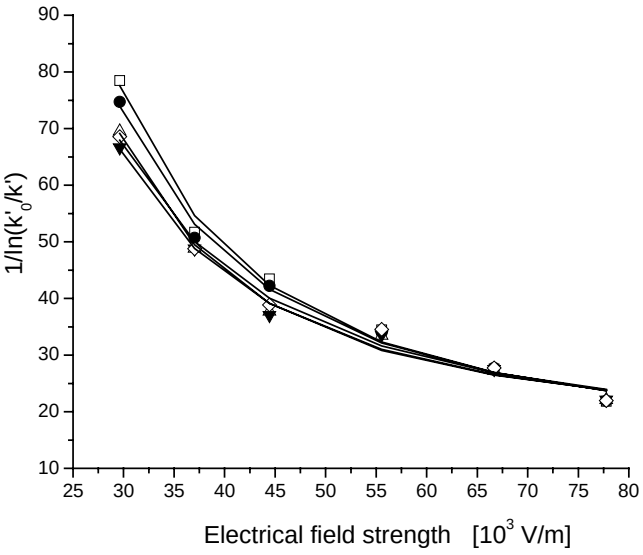


Fig. 4. Effect of Joule heating on the retention factor in CEC with a polymeric monolithic stationary phase. Column: polymethacrylate ester-based monolith, 27 cm (20 cm effective); mobile phase: acetonitrile–Tris (pH 8.7) (80:20, v/v) with an effective Tris concentration of 5 mM; analytes: benzene (□), toluene (●), propylbenzene (△), butylbenzene (▼), and amylbenzene (◇). Solid lines: best fits of the data to Eq. (17).

Table 3
Best fitting parameters of Eq. (17)

| Separation mode | Compound | Parameters | | |
|---|---|---|---|---|
| | | $A$ ($10^{-3}$ K$^2$m/V) | $i$ | $B$ |
| Particulate CEC | Methylbenzoate | 0.76 | 2.26 | 1.72 |
| | Ethylbenzoate | 0.16 | 2.64 | 1.27 |
| Monolithic CEC | Benzene | 1.39 | 2.05 | 15.03 |
| | Toluene | 2.10 | 1.94 | 14.59 |
| | Propylbenzene | 1.27 | 2.13 | 17.20 |
| | Butylbenzene | 2.73 | 1.91 | 15.78 |
| | Amylbenzene | 3.18 | 1.85 | 15.09 |

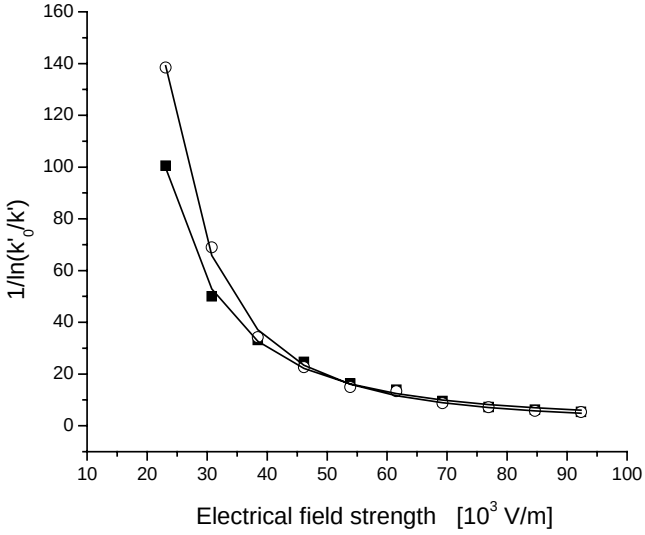


Fig. 5. Effect of Joule heating on the retention factor in CEC with a particulate stationary phase. Column: 32.5 cm (24 cm effective), Purospher STAR 400-ODS ($d_p$ = 2.45 μm); mobile phase: acetonitrile–Tris (pH 8.3) (80:20, v/v) with an effective Tris concentration of 40 mM; applied voltage: 20 kV; analytes: methylbenzoate (■), ethylbenzoate (○). Solid lines: best fits of the data to Eq. (17).

reciprocal of the standard enthalpy of solute transfer from the mobile to the stationary phase. The smaller this parameter, the more negative the standard enthalpy, meaning that differences in the bonding energy between solute–stationary phase and solute–mobile phase are greater under the CEC conditions with the studied particulate columns which is, of course, also seen in the different $k'$-values. The parameter $i$ shows the strength of the Joule heating effect on electrical conductivity of the mobile phase with applied field strength (closely related to the temperature rise in the electrolyte), leading to lower retention factors of the solute. The slightly higher values of $i$ in particulate than monolithic CEC indicates more severe Joule heating, which is in agreement with the stronger decrease in retention factors of alkylbenzoates at increasing electrical field strength under particulate CEC conditions (Table 2) caused by the higher effective ionic strength (40 mM versus 5 mM) and a larger diameter of the used capillary (100 μm versus 75 μm).

### 3.4. Effect of Joule heating on column efficiency

The radial temperature distribution in the electrolyte over the column cross-section exhibits a parabolic-like (or nearly so) pattern [25,26]. The highest temperature occurs at the capillary centerline suggesting that generated Joule heat is transferred from the central region to the wall by convection and then dissipated through the capillary wall by conduction. Temperature variations across the column result in a macroscopically inhomogeneous velocity profile for the solute band as a whole and tend to engender additional dispersion. On the other hand, transverse diffusion (or actually, transverse dispersion) counteracts this axially-dispersive tendency. For effective radial dispersion mechanisms and small channel dimensions, the influence of the almost parabolic flow profile on the overall band broadening becomes less significant in that molecules in the high-velocity region in the capillary center will be equilibrated faster with those in the low-velocity region at the wall. Eventually, a Gaussian solute band (characterized by an increased axial dispersion coefficient) develops along the axis of the capillary under the influence of these effects. The thermal contribution by the radial temperature profile to the plate height, $H_{th}$, can be described as [3]:

$$H_{th} = 10^{-8} \frac{\varepsilon_0 \varepsilon_r \lambda_D}{D_m \eta k^2} E^5 d_c^6 \kappa^2 c^2 \quad (18)$$

where $\lambda_D$, $D_m$, $k$, $d_c$, $\kappa$ and $c$ denote the electrical double layer thickness, diffusion coefficient of solute in free solution, thermal conductivity, column bore diameter, the molar conductivity of the solution, and electrolyte concentration.

It should be remembered that, even if the macroscopic flow maldistribution appears to be negligible, the remaining average temperature increase in the capillary lumen due to the Joule heating also has a profound influence on the separation efficiency via an increase in the diffusion coefficient. Indeed, within a moderate temperature range, the decrease in separation efficiencies is mostly caused by the increased axial diffusion of the analyte molecules [17,27].

In CEC packed with wide-pore particles, the intraparticle EOF can be significantly enhanced which results in a higher pore-to-interstitial flow ratio due to the dominating effect of intraparticle electrical double layer overlap-suppression at an increasing Tris concentration. Thus, increasing intraparticle EOF improves the flow homogeneity over the column cross-section (in a global sense) and decreases mass transfer resistance in the mobile and stationary phases [28,29]. Fig. 6 shows that the height equivalent to a theoretical plate ($H$) decreases with an increase of the Tris buffer concentration from 0.1 to 10 mM, which can be attributed to the electroosmotic perfusion mechanism [30–32] and the equilibrium effect [28,29]. However, with a further increase of the Tris concentration to 40 mM within this series (Fig. 6), plate height increases and column efficiency decreases which can be explained by the actual power dissipation in the packed capillary, leading to development of Joule heat. This causes an (uncorrected) increase of the analytes diffusion coefficient in the bed which, because the dispersion data are acquired in the diffusion-limited regime, is seen in higher axial dispersivities $D_{ax}/D_m$ (Fig. 7) [33]. At higher buffer concentrations, the plate height may be thought of being composed of several independent contributions, i.e., the “eddy flow” term, axial diffusion, mass transfer kinetics in the stationary and mobile phases, and the Joule heating effect. The finite rate of heat transfer at higher buffer concentrations plays an important role in a decrease of column efficiency in CEC with small adsorbent particles (for which the diffusion-limited regime can be hardly left) as it causes an increase of the

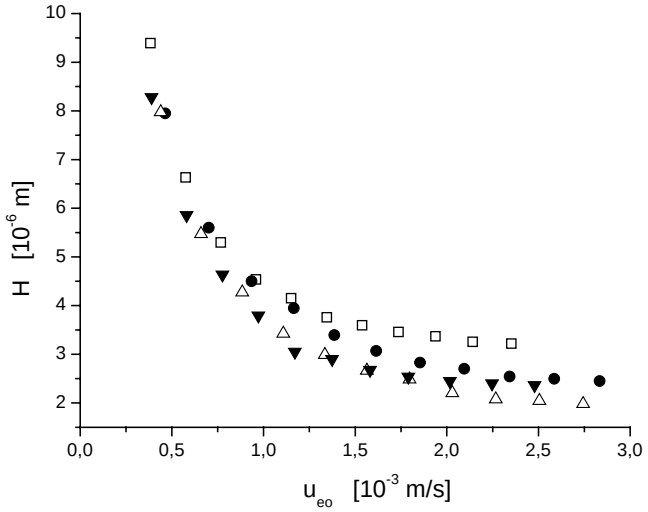


Fig. 6. Effect of buffer concentration on the plate height of methylbenzoate vs. the EOF velocity in perfusive CEC. Column packing: Purospher STAR 1200-ODS ($d_p = 2.46\,\mu m$); mobile phase: acetonitrile–Tris (pH 8.3) (80:20, v/v); 0.1 mM (□), 1.0 mM (●), 10.0 mM (△) and 40.0 mM (▼) effective Tris concentration.

molecular diffusivity depending on the average temperature in the column. However, when this temperature increase is less than 25 °C, the radial temperature gradients are small and the associated Taylor dispersion can become negligible [15,17]. Thus, within a moderate temperature range, the contribution of a macroscopic EOF velocity profile (arising from radial temperature gradients) to the separation efficiency is insignificant and the Joule heating is mainly manifested in an increased axial diffusion term for the overall plate height.

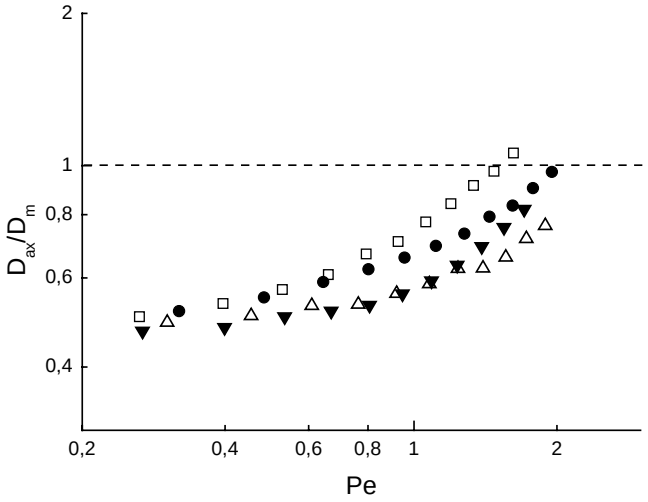


Fig. 7. Effect of buffer concentration on the axial dispersivity $D_{ax}/D_m$ (ratio of apparent axial dispersion coefficient to free molecular diffusion coefficient of analyte in mobile phase) of methylbenzoate vs. the particle Péclet number, $Pe = u_{eo}d_p/D_m$. Experimental conditions as in Fig. 6.

## 4. Conclusions

General acceptance of CEC and scale-up of electrochromatographic separations have been problematic due to electrically-induced heating, i.e., the Joule heating effect. Slow heat transfer to the surrounding environment through the capillary wall results in radial temperature gradients inside the column which can result in a pronounced parabolic (or nearly so) flow profile but, for only moderate Joule heating, mainly causes a homogeneous increase of the mobile phase temperature. For the systems studied, as the mobile phase Tris concentration is above 5.0 mM (and the accompanying power level exceeds about 0.35 W/m), the Joule heating effect cannot be neglected any longer. The model analysis presented in this article, Eq. (9), can be used to predict the dependence of the EOF velocity on applied electrical field strength in the presence of Joule heating. The parameter L in this model is important for extrapolation of the EOF velocity without Joule heating, while the parameters $M$ and $\theta$ quantify its contribution. Further, Eq. (17) provides a dependence of the retention factor of a solute on applied electrical field strength under the influence of Joule heating. Lastly, for moderate Joule heating, additional band broadening introduced by the macroscopic flow profile arising from radial temperature gradients becomes insignificant, and its effect on separation efficiency is mainly manifested in the increased axial diffusion caused by the actual low-Péclet-number hydrodynamics.

## Acknowledgements

We are grateful to Dieter Lubda from Merck KGaA (Darmstadt, Germany) for the preparation of particle research samples and further acknowledge financial support by the Landesgraduiertenförderung Sachsen-Anhalt (Germany) to Guofang Chen.

## References

[1] J.H. Knox, I.H. Grant, Chromatographia 32 (1991) 317.
[2] R.J. Boughtflower, T. Underwood, C.J. Paterson, Chromatographia 40 (1995) 329.
[3] J.H. Knox, Chromatographia 26 (1988) 329.
[4] J.H. Knox, K.A. McCormack, Chromatographia 38 (1994) 207.
[5] J.H. Knox, K.A. McCormack, Chromatographia 38 (1994) 215.
[6] A.S. Rathore, K.J. Reynolds, L.A. Colón, Electrophoresis 23 (2002) 2918.
[7] G.Y. Tang, C. Yang, J.C. Chai, H.Q. Gong, Int. J. Heat Mass Transfer 47 (2004) 215.
[8] C. Keim, M. Ladisch, AIChE J. 49 (2003) 402.
[9] R.F. Cross, J. Cao, J. Chromatogr. A 809 (1998) 159.
[10] R.F. Cross, J. Chromatogr. A 907 (2001) 357.
[11] S. Palonen, M. Jussila, S.P. Porras, T. Hyötyläinen, M. Riekkola, J. Chromatogr. A 916 (2001) 89.
[12] K. Swinney, D.J. Bornhop, Electrophoresis 23 (2002) 613.
[13] S. Palonen, S.P. Porras, M. Jussila, M. Riekkola, Electrophoresis 24 (2003) 1565.

[14] S.P. Porras, E. Marziali, B. Gaš, E. Kenndler, Electrophoresis 24 (2003) 1553.
[15] U. Tallarek, E. Rapp, T. Scheenen, E. Bayer, H. Van As, Anal. Chem. 72 (2000) 2292.
[16] M.E. Lacey, A.G. Webb, J.V. Sweedler, Anal. Chem. 72 (2000) 4991.
[17] K.-L.K. Liu, K.L. Davis, M.D. Morris, Anal. Chem. 66 (1994) 3744.
[18] L. Yu, J.M. Davis, Electrophoresis 16 (1995) 2104.
[19] T.H. Seals, J.M. Davis, M.R. Murphy, K.W. Smith, W.C. Stevens, Anal. Chem. 70 (1998) 4549.
[20] G. Chen, U. Tallarek, Langmuir 19 (2003) 10901.
[21] G. Ping, P. Schmitt-Kopplin, N. Hertkorn, W. Zhang, Y. Zhang, A. Kettrup, Electrophoresis 24 (2003) 958.
[22] A.S. Rathore, Cs. Horváth, J. Chromatogr. A 781 (1997) 185.
[23] A.S. Rathore, Cs. Horváth, Anal. Chem. 70 (1998) 3069.
[24] M.S. Bello, M. Chiari, M. Nesi, P.G. Righetti, M. Saracchi, J. Chromatogr. 625 (1992) 323.
[25] E. Grushka, R.M. McCormick, J.J. Kirkland, Anal. Chem. 61 (1989) 241.
[26] A.E. Jones, E. Grushka, J. Chromatogr. 466 (1989) 219.
[27] J.M. Davis, J. Chromatogr. 517 (1990) 521.
[28] R. Stol, H. Poppe, W.Th. Kok, Anal. Chem. 73 (2001) 3332.
[29] H. Poppe, R. Stol, W.Th. Kok, J. Chromatogr. A 965 (2002) 75.
[30] E. Wen, R. Asiaie, Cs. Horváth, J. Chromatogr. A 855 (1999) 349.
[31] U. Tallarek, M. Pačes, E. Rapp, Electrophoresis 24 (2003) 4241.
[32] P.T. Vallano, V.T. Remcho, Anal. Chem. 72 (2000) 4255.
[33] G. Chen, M. Pačes, M. Marek, Y. Zhang, A. Seidel-Morgenstern, U. Tallarek, Chem. Eng. Technol. 27 (2004) 417.